BMC Genomics

RESEARCH

Open Access

Transcriptomic and proteomic studies of body size and carcass traits and the longest dorsal muscle in Tibetan sheep

Dehui Liu[1,2,4], Xue Li[1], Lei Wang[3], Quanbang Pei[3], Jincai Zhao[3], De Sun[6], Qianben Ren[3], Buying Han[1], Hanjing Jiang[5], Wenkui Zhang[3], Rong Li[7], Guoxiang Bao[8], Song Wang[1,2], Fei Tian[1], Sijia Liu[1], Kai Zhao[1] and Dehong Tian[1*]

Abstract

Background Tibetan sheep represent valuable genetic resources on the Tibetan Plateau, and their body size and carcass traits serve as crucial foundations for breeding program development and breeding effects evaluation. The study of body size and carcass characteristics of Tibetan sheep helps to understand their process of genetic regulation.

Result The body size traits, carcass traits, and muscle fiber structure of plateau-type Tibetan and Zhashijia sheep were compared. Zhashijia ewes displayed considerably higher carcass weight and body size than plateau-type ewes. Additionally, it was observed that Zhashijia rams exhibited significantly greater eye muscle area, chest width, and muscle fiber perimeter in comparison to plateau-type rams. And Glycogen staining results showed that the glycogen content of the plateau-type Tibetan sheep was significantly higher than that of the Zhashijia sheep. Through transcriptomic and proteomic analyses, we identified 366 genes that showed differential expression in the ram group and 248 proteins with differential expression. In the ewe group, we found 623 differentially expressed genes (DEGs) and 624 differentially expressed proteins (DEPs). Among these, eleven genes and fourteen proteins were associated with body size and carcass quality. These genes and proteins showed significant enrichment in the PPAR signaling pathway and protein digestion and absorption. Furthermore, employing weighted gene co-expression network analysis (WGCNA) allowed us to identify twelve genes that are pivotal in regulating body size and carcass. Finally, RT-qPCR validation confirmed the reliability of our RNA-Seq results.

Conclusion The findings of this study contribute to a deeper comprehension of the morphological characteristics and carcass traits of Tibetan sheep, thereby establishing a robust scientific basis for the selective breeding of novel sheep breeds with enhanced growth performance and superior meat production capacity.

Keywords Body size traits, Carcass traits, Proteomics, Tibetan sheep, Transcriptomics, WGCNA

*Correspondence:
Dehong Tian
tiandehong@nwipb.cas.cn
Full list of author information is available at the end of the article

Background

In sheep breeding, body size and carcass traits represent crucial economic traits in meat sheep and display complex quantitative inheritance patterns with moderate to high heritability [1–4]. These traits play a pivotal role in selection programs aimed at enhancing growth rates and improving carcass quality [5, 6]. Tibetan sheep (*Ovis aries*), predominantly distributed across the Tibetan Plateau, demonstrate a unique genetic structure and significant geographic adaptability [7]. The plateau-type Tibetan sheep (PT) and Zhashijia sheep (ZS) represent two distinct ecotypes of Tibetan sheep. Notably, the PT is renowned for its superior meat quality, whereas the ZS exhibits greater body weight and more pronounced size characteristics. Both ecotypes possess unique production performance and biological traits. Leveraging these two distinct ecotypes provides an optimal framework for investigating the fundamental regulatory mechanisms underlying sheep growth and meat production performance. Consequently, we conducted comprehensive transcriptome and proteome analyses on the longest dorsal muscle tissues obtained from PT and ZS to identify potential biomarkers associated with growth performance and carcass traits.

It has been reported that gene expression influence growth and development in farm animals. Through the transcriptomic comparison of breast and leg muscles between local chicken breeds, Liu et al. 2024 identified that genes related to the PPAR signaling pathway were differentially expressed, which were associated with distinct growth phenotypes in local breeds and broilers [8]. Ding et al. 2021 identified 20 potential candidate genes associated with skeletal muscle development and growth in pigeons using transcriptome and weighted gene co-expression network analysis [9]. These findings suggest that transcriptome analysis could be an effective tool for screening markers for future molecular breeding. Comprehending muscle growth and development mechanisms is imperative for enhancing meat yield and quality. However, it should be emphasized that muscle growth and development constitute a complex multi-step regulatory process necessitating meticulous investigation. Recent research has unveiled the immense potential of proteomics in unraveling the intricate regulatory processes governing muscle growth and development. Zhao et al. 2022 identified five proteins associated with fat synthesis and muscle development, namely ILK, AHCYL2, MLIP, CYB5A, and SMTNL1, through proteomic analysis of the longest and shortest muscles in the thoracic region of the Hu and Dorper sheep. These differentially abundant proteins are potential candidate markers for predicting body weight in sheep. Fat deposition and muscle growth are critical determinants of sheep body weight variation [10]. The transcriptome explores differential genes with specific biological functions and elucidates gene networks and pathways, providing insights into the organism's activities. Proteins are vital mediators of life processes and fundamental units that execute the functions of living organisms. They form intricate pathway networks by assembling into various complexes, performing multiple biological functions, and revealing the organism's past events. The correlation coefficients between transcriptome-proteome levels in different tissues ranged from 0.3 to 0.5 [11]; therefore, studying mRNA expression alone cannot sufficiently explain variations in protein levels. By integrating transcriptome and proteome data, linking mRNA expression levels with protein abundance through comprehensive analysis, and exploiting the disparities and complementarities between transcriptomics and proteomics studies, we can comprehensively analyze gene expression levels, uncover gene interaction networks, and subsequently decipher the biological function of individual genes to capture dynamic changes in growth and development processes.

In this study, we employed integrated morphological, transcriptomic, and proteomic analyses along with WGCNA to identify key genes and proteins associated with body size and carcass characteristics traits between PT and ZS. These findings will contribute to enhancing breed selection strategies for improved production performance, meeting the increasing demands of breeders, and accelerating the achievement of breeding goals.

Results

Determination of production performance of Tibetan sheep

The production performance was evaluated in PT and ZS sheep. The comparative analysis of body size and carcass traits revealed that ZS rams exhibited significantly higher values for body height (BH), body length (BL), chest circumference (CC), chest depth (CD), pipe circumference (PC), chest width (CW), carcass weight (CaW), and eye muscle area (EMA) compared to PT rams ($P<0.05$ and $P<0.01$) (Tables 1 and 2). In ewes, ZS demonstrated significantly greater ($P<0.01$) values for body height (BH), body length (BL), chest circumference (CC), chest depth (CD), chest width (CW), live weight (LW), and carcass weight (CaW) than PT (Tables 3 and 4). These results indicated ZS showed better performance in both body size and carcass traits than PT.

Furthermore, the present study analyzed and compared the muscle fiber characteristics of the two Tibetan sheep. ZS rams demonstrated significantly greater muscle fiber perimeter compared to PT rams ($P<0.05$) (Fig. 1 and Table 5).

Table 1 Comparison of body size of PT rams and ZS rams

Variety	N	BH	BL	CC	CD	CW	WW	PC
PT	4	63.15 ± 1.96	58.98 ± 3.46	78.83 ± 4.40	27.15 ± 1.21	18.40 ± 1.17	12.18 ± 0.47	7.15 ± 0.17
ZS	5	70.90 ± 4.34*	68.60 ± 5.22*	88.76 ± 7.13*	31.60 ± 2.97*	24.50 ± 2.67**	12.70 ± 1.20	8.26 ± 0.69*

BH Body Height, *BL* Body Length, *CC* Chest Circumference, *CW* Chest Width, *CD* Chest Depth, *WW* Waist angle Width, *PC* Pipe Circumference. The phenotypic values are the mean ± standard error (SE). Different superscript lowercase letters * within a row indicate significant differences at significance levels between $0.01 < P < 0.05$, and ** indicates significant differences at $P < 0.01$

Table 2 Comparison of carcass traits of PT rams and ZS rams

Variety	N	LW	CaW	EMA	BT	GR
PT	4	30.88 ± 1.93	12.31 ± 1.37	10.13 ± 1.35	1.30 ± 0.53	1.39 ± 0.44
ZS	5	33.84 ± 2.74	15.98 ± 1.52**	14.10 ± 2.96*	1.08 ± 0.42	1.72 ± 0.77

LW Live Weight, *CaW* Carcass Weight, *EMA* Eye Muscle Area, *BT* Backfat Thickness. Different superscript lowercase letters * within a row indicate significant differences at significance levels between $0.01 < P < 0.05$, and ** indicates significant differences at $P < 0.01$

Table 3 Comparison of body size of PT ewes and ZS ewes

Variety	N	BH	BL	CC	CD	CW	WW	PC
PT	5	57.62 ± 2.73	58.00 ± 1.84	76.74 ± 3.42	25.96 ± 1.80	18.56 ± 0.59	11.66 ± 0.73	6.86 ± 0.09
ZS	5	70.20 ± 2.86**	66.10 ± 2.30**	88.80 ± 3.55**	31.90 ± 2.13**	24.30 ± 0.67**	11.60 ± 1.34	7.54 ± 0.68

BH Body Height, *BL* Body Length, *CC* Chest Circumference, *CW* Chest Width, *CD* Chest Depth, *WW* Waist angle Width, *PC* Pipe Circumference. The phenotypic values are the mean ± standard error (SE). Superscript lowercase letters ** indicate highly significant differences ($P < 0.01$)

Table 4 Comparison of carcass traits of PT ewes and ZS ewes

Variety	N	LW	CaW	EMA	BT	GR
PT	5	26.20 ± 1.10	11.27 ± 0.46	10.28 ± 1.35	0.89 ± 0.19	1.21 ± 0.29
ZS	5	32.96 ± 1.39**	14.44 ± 1.07**	11.14 ± 1.14	1.27 ± 0.93	1.77 ± 0.78

LW Live Weight, *CaW* Carcass Weight, *EMA* Eye Muscle Area, *BT* Backfat Thickness. Superscript lowercase letters ** indicate highly significant differences ($P < 0.01$)

Transcriptomic analysis

In the transcriptomics analysis, 472,997,652 and 502,666,826 high-quality clean reads were obtained from PT and ZS, which yielded a mapping ratio of 98.74% and 98.61%, which ensured subsequent quantitative analyses. The mean values of Q20 and Q30 for the PT sample were 98.17% and 96.55%, respectively, while those for the ZS sample were 98.05% and 96.44%, respectively (Supplementary Table 1).

Through transcriptome analysis, we identified 366 DEGs in the comparison between PT and ZS rams, including the up- and down-regulation of 225 and 141 genes, respectively. Similarly, 623 DEGs were identified between PT and ZS ewes, including 240 up-regulated and 383 down-regulated genes (Fig. 2A-B). The heatmap analysis revealed distinct gene expression profiles between the two breeds in both genders (Fig. 2C-D). Additionally, we found 77 genes were commonly differentially expressed between two breeds (Supplementary Fig. 1A).

GO and KEGG enrichment analysis of DEGs

To understand the function of DEGs, both GO and KEGG enrichment analyses were performed. DEGs in ram and ewe were overrepresented in 443 and 785 GO terms, respectively (Supplementary Table 2 and Fig. 3A-B). Among these GO terms, we found that glycogen metabolic processes, animal organ development, system development, muscle organ development, muscle structure development, and skeletal system development were enriched in both genders.

DEGs from rams and ewes were highly represented in 23 and 28 pathways, respectively (Supplementary

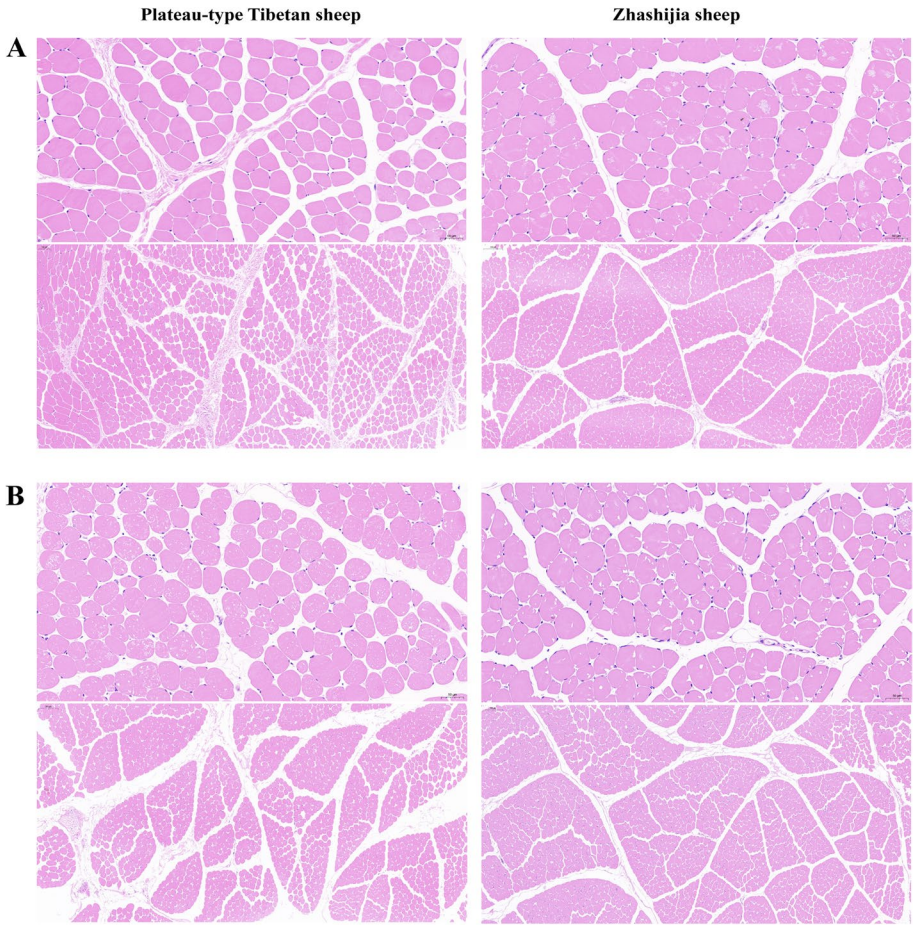

Fig. 1 The tissue section of the longest dorsal muscle. A represents a histological section of the longest dorsal muscle stained with hematoxylin and eosin (HE) in PT and ZS; B represents a histological section of the longest dorsal muscle stained with HE in PT ewes and ZS ewes

Table 5 Determination of muscle fiber characteristics in PT and ZS

	PT		ZS	
N	**4**	**5**	**5**	**5**
Gender	male	female	male	female
Diameter of muscle fibers (mm)	0.054 ± 0.002	0.061 ± 0.002	0.064 ± 0.004	0.066 ± 0.003
Perimeter of muscle fibers (mm)	0.186 ± 0.008	0.215 ± 0.009	0.232 ± 0.016*	0.238 ± 0.014
Area of muscle fibers (mm^2)	0.368 ± 0.020	0.392 ± 0.008	0.394 ± 0.009	0.384 ± 0.015
Density of muscle fibers (Piece/mm^2)	419.355 ± 39.257	344.816 ± 25.953	307.532 ± 39.592	305.736 ± 24.397
Number of muscle fibers (Piece)	153.000 ± 15.000	136.000 ± 12.000	119.000 ± 12.000	116.000 ± 8.000

The phenotypic values are the mean ± standard error (SE). *P*-values were calculated using a t-test. Different superscript lowercase letters * within a row indicate significant differences at significance levels between $0.01 < P < 0.05$

Table 3 and Fig. 3C-D). Among these pathways, we found significant enrichment in the AMPK signaling pathway, Cardiac muscle contraction, steroid hormone biosynthesis, and specific amino acid metabolic pathways.

Reverse transcription-quantitative PCR (RT-qPCR) validation

We employed the RT-qPCR method to assess the mRNA levels of 11 DEGs to validate the transcriptomics data. The results depicted in Fig. 4, which demonstrated a consistent expression pattern between RT-qPCR and RNA

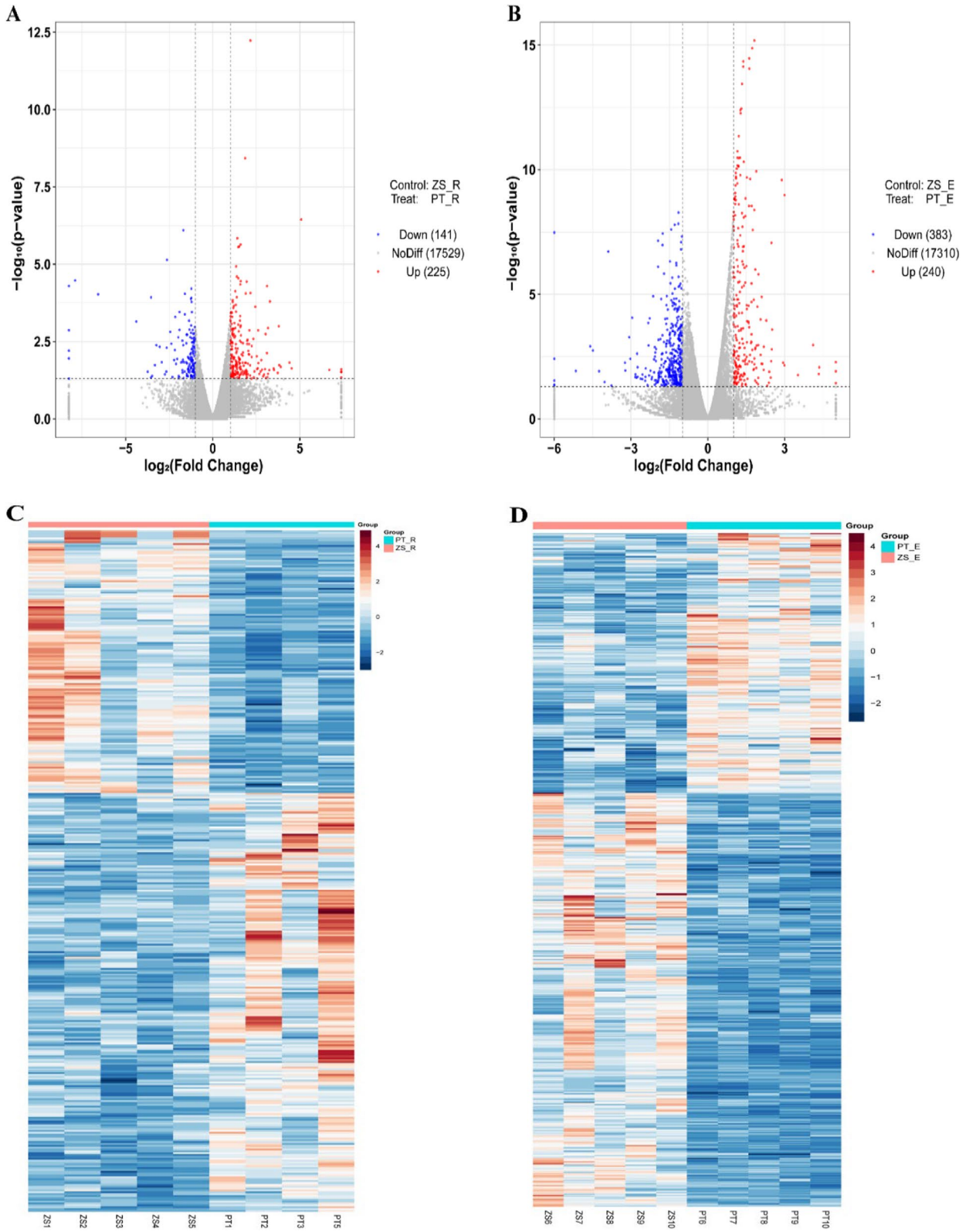

Fig. 2 Differentially expressed genes (DEGs) were analyzed to compare PT and ZS. **A**, **B** A volcano plot was generated to visualize the DEGs. Red dots indicate upregulated DEGs, blue dots represent downregulated DEGs and grey dots indicate no significant change between groups. **C, D** Heatmaps of DEGs. The PT_R category comprises PT1-4 as plateau-type rams, while the ZS_R category includes ZS1-5 as Zhashijia rams. Similarly, the PT_E category consists of PT5-9 as plateau-type ewes and the ZS_E category includes ZS6-10 as Zhashijia ewes

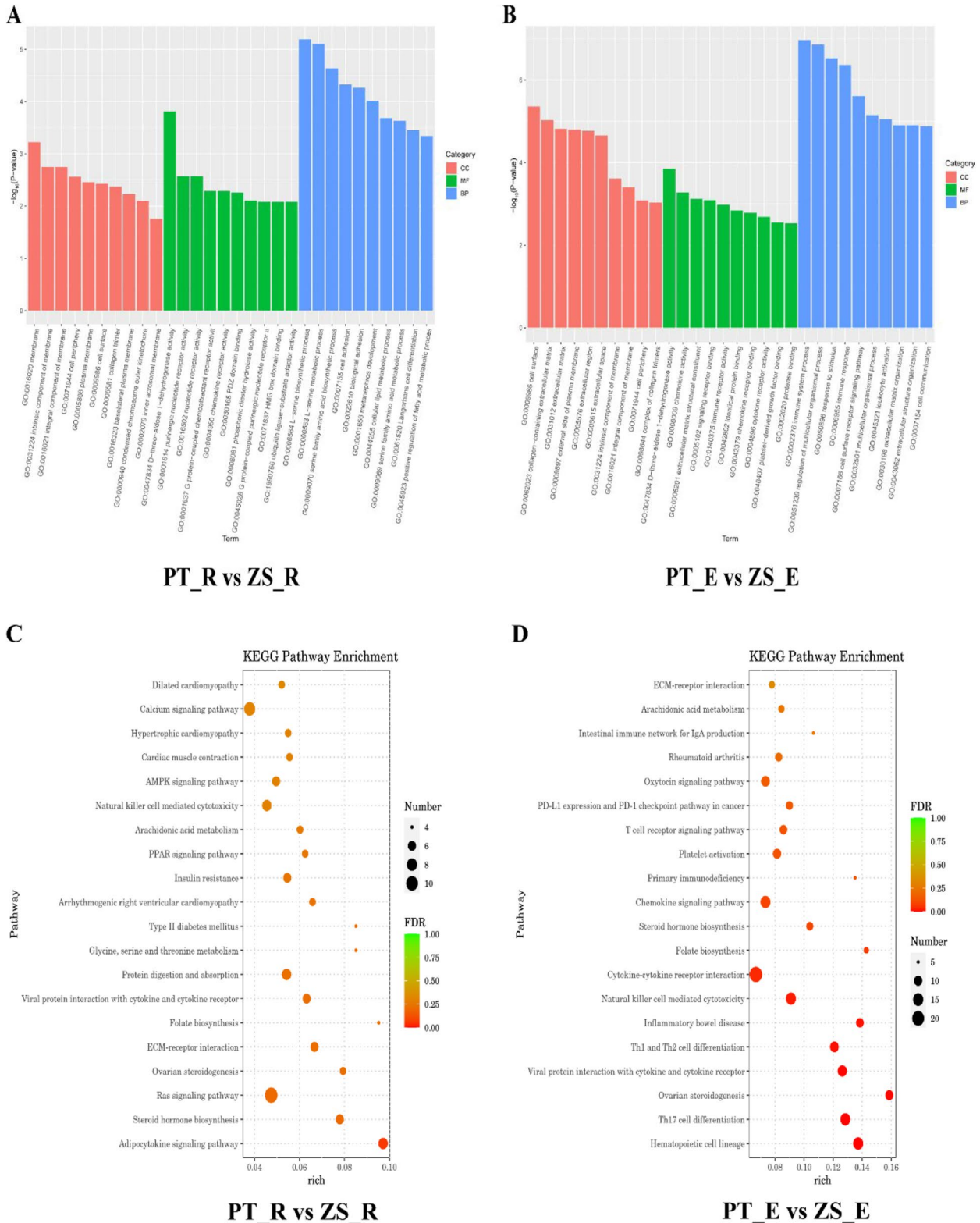

Fig. 3 Functional enrichment analysis of differentially expressed genes (DEGs). **A** GO term enrichment of DEGs in PT_R (ram) versus ZS_R (ram); (**B**) GO term enrichment of DEGs in PT_E (ewe) versus ZS_E (ewe); (**C**) KEGG analysis of DEGs in PT_R (ram) versus ZS_R (ram). (D) KEGG analysis of DEGs in comparing PT_E (ewe) and ZS_E (ewe)

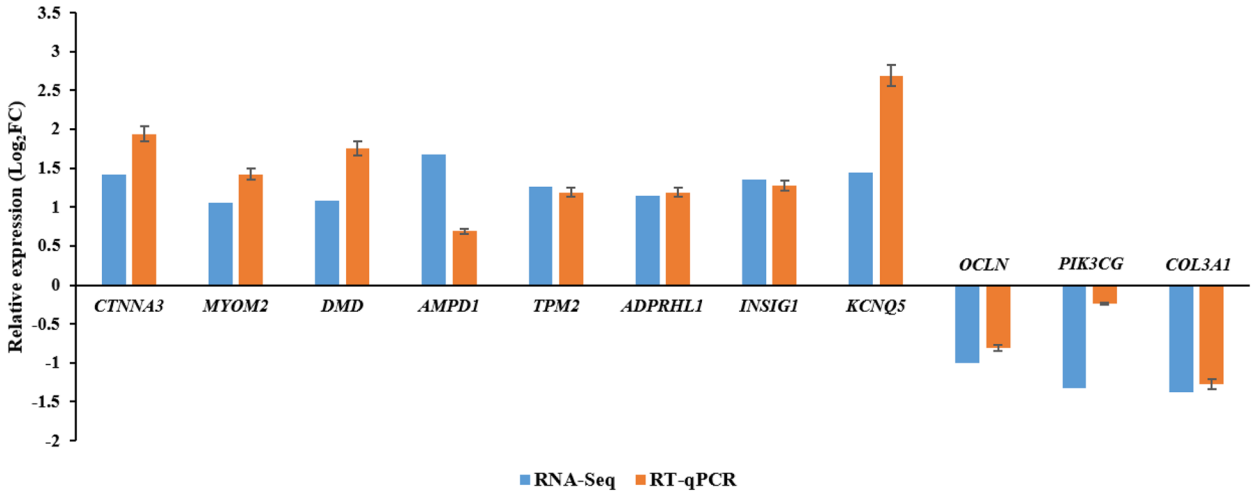

Fig. 4 Validation of RNA-Seq by RT-qPCR analysis. RNA-Seq results are shown in blue and RT-qPCR results are shown in orange

sequencing data, with a Pearson correlation coefficient of 0.87. This effectively validates the findings of RNA-seq analysis, further reinforcing the reliability of transcriptome analysis.

Proteomics analysis

In the proteomics analysis, 33,901 peptides and 5128 proteins were identified from all PT samples, while 35,419 peptides and 5168 proteins were identified from ZS samples. The proteomic analysis revealed a total of 248 DEPs in PT rams compared to ZS rams, with 91 up-regulated and 157 down-regulated (Fig. 5A). Similarly, a total of 624 DEPs were detected in PT ewes relative to ZS ewes, with 68 up-regulated and 556 down-regulated (Fig. 5B). The composite heatmap analysis revealed a significant disparity in the expression of differential proteins, encompassing 43 DEPs between two genders (Fig. 5C-D and Supplementary Fig. 1B).

GO and KEGG enrichment analysis of DEPs

We observed a significant enrichment of DEPs at the proteomic level in 75 GO terms when comparing PT rams with ZS rams. Similarly, a considerable abundance enrichment of DEPs was found in 114 GO terms when comparing PT ewes with ZS ewes (Supplementary Table 4 and Fig. 6A-B). Comprising tissue development, GTP biosynthetic process, and cytoskeleton organization.

At the protein level, 20 significantly enriched pathways were identified in the PT_R vs. ZS_R comparison, and 54 significantly enriched pathways were identified in the PT_E vs. ZS_E (Supplementary Table 5 and Fig. 6C-D). Differential proteins were mainly enriched in fatty acid metabolism, amino acid biosynthesis, and the HIF-1 signaling pathway. Transcriptomic and proteomic analyses have revealed two identical pathways, the PPAR signaling pathway and protein digestion and absorption.

Correlation between transcriptome and proteome

In the present study, the integrated analysis of transcriptome and proteomics revealed that six genes/proteins (up-regulated trends) exhibited a consistent expression pattern in the ram group, with ALB, COL14A1, CSRP3, EYA1 and MYOM3 located in the third quadrant and CD200 in the seventh quadrant. In contrast, twelve genes/proteins (down-regulated trends) displayed a similar expression trend within the ewe group, including C25H10orf71, COL23A1, and PADI2, found in the third quadrant, and C8B, F9, KIF4A, LOC101117129, NCKAP5, OCLN, PON1, QSOX1 and TNC were observed in the seventh quadrant (Fig. 7). The correlation coefficient between the PT_R vs. ZS_R transcriptome and proteome was 0.04, while for the PT_E vs. ZS_E transcriptome and proteome, it was 0.06, indicating a positive but relatively weak correlation between the transcriptomic and proteomic results. The main reason for the low correlation may be that the two histological analyses were performed separately, and the interaction between mRNAs and proteins is affected by changes in translation efficiency and mRNA expression levels [12]. The flip-flop process from mRNA to protein is very complex, and factors such as mRNA splicing and protein degradation may lead to poor correlation between the transcriptome and proteome [13].

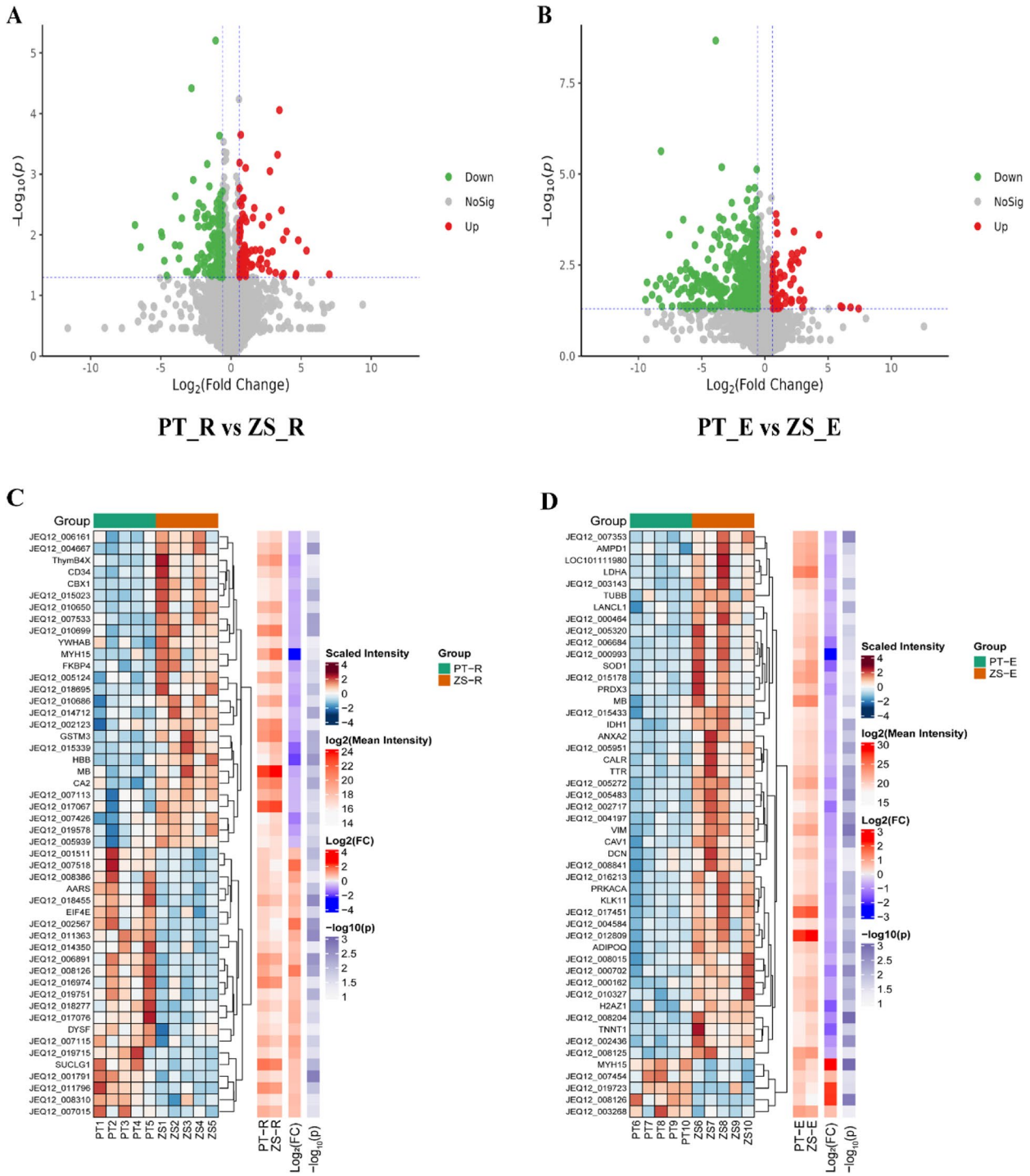

Fig. 5 Differentially expressed proteins (DEPs) were analyzed to compare PT and ZS. **A, B** A volcano plot was generated to visualize the DEPs. Red dots indicate upregulated DEP, green dots represent downregulated DEPs, and grey dots indicate no significant change between groups. **C, D** Complex heatmaps of DEPs. The PT_R category comprises PT1-5 as plateau-type rams, while the ZS_R category includes ZS1-5 as Zhashijia rams. Similarly, the PT_E category consists of PT6-10 as plateau-type ewes and the ZS_E category includes ZS6-10 as Zhashijia ewes

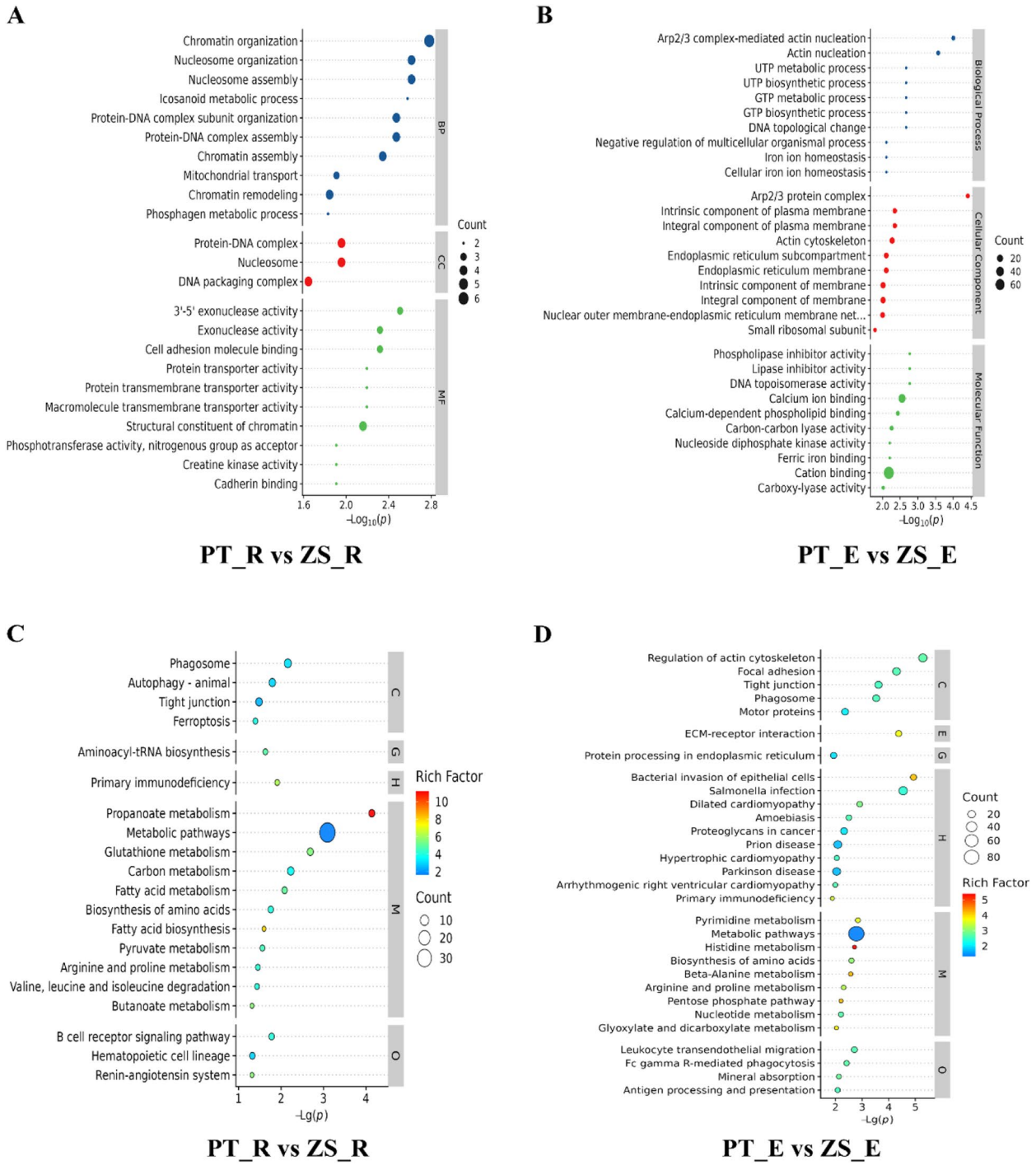

Fig. 6 Functional enrichment analysis of differentially expressed proteins (DEPs). **A** GO term enrichment of DEPs in PT_R (ram) versus ZS_R (ram); (**B**) GO term enrichment of DEPs in PT_E (ewe) versus ZS_E (ewe); (**C**) KEGG analysis of DEPs in PT_R (ram) versus ZS_R (ram). **D** KEGG analysis of DEPs in comparing PT_E (ewe) and ZS_E (ewe)

WGCNA for transcriptomics

The scale-free fit index and mean connectivity were calculated using the soft threshold power of $\beta = 14$. The observation that the scale-free $R^2 > 0.8$ and mean connectivity tends to zero indicates that utilizing the power of $\beta = 14$ for network construction enables the formation of a scale-free network (Supplementary Fig. 2B). The selected genes were clustered using a dissimilarity

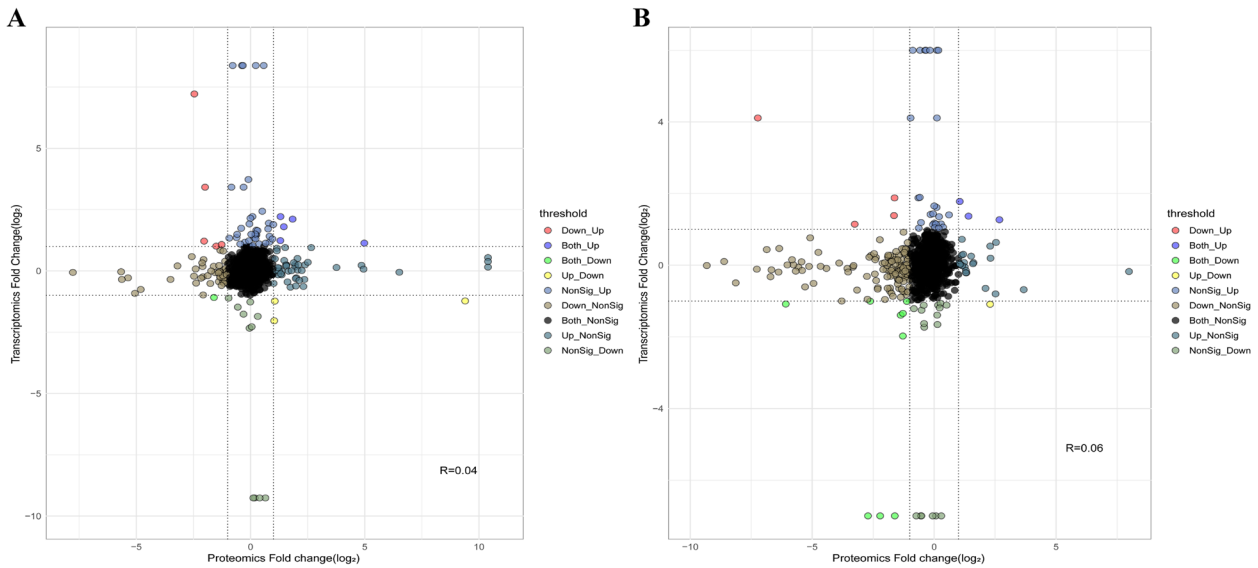

Fig. 7 Correlation analysis of transcriptomes and proteomes was performed. **A** The correlation between transcripts (y-axis) and proteins (x-axis) was examined in the PT_R vs. ZS_R comparison. **B** The correlation between transcripts (y-axis) and proteins (x-axis) was investigated in the PT_E vs. ZS_E comparison. Note: The x-axis represents the log_2FC of proteins while the y-axis represents the log_2FC of genes. Significant changes in expression are color-coded

measure based on a topological overlap matrix (TOM). This measure was derived from a dynamic tree-cutting algorithm, resulting in partitioning the dynamic tree into 23 distinct modules, each characterized by unique colors (Supplementary Fig. 2C). The interactions between these co-expression modules were subsequently analyzed using Pearson correlation coefficients. The modules in the cluster analysis underwent hierarchical clustering of feature genes. The dendritic graph branches (meta-modules) were grouped based on the correlation of these genes (Supplementary Fig. 2D). Each module represents a distinct gene cluster and is visually differentiated by various colors in the topologically overlapping heatmap: red indicating positive correlation and blue indicating negative correlation (Supplementary Fig. 2A).

The module-phenotype (including gender) correlation analysis identified significant correlation ($p < 0.01$) between six modules with body size traits. Lightcyan module displayed substantial and positive correlations with CW, while brown showed such correlations with LW, CW, PC, CaW, and GR value ($p < 0.01$). Purple exhibited highly significant and positive correlations with a perimeter of muscle fibers ($p < 0.01$). Green similarly displayed high importance in its positive correlation with BL, CC, and CD ($p < 0.01$); grey exhibited a remarkable correlation with both LW and BH; finally, turquoise was observed to have a highly significant and positive relationship specifically towards LW, BH, BL, CD, CW, CC, and CaW ($p < 0.01$) (Fig. 8).

Analysis of critical modular genes and enrichment associated with body size and carcass

We identified six modules that significantly correlated with phenotypes through module-phenotype correlation analysis, namely lightcyan, brown, purple, green, grey and turquoise. Subsequently, we conducted enrichment analysis on the genes within these six modules. We observed significant enrichments in macromolecule metabolic process, positive regulation of muscle hypertrophy, Some glycogen metabolism, and bone development terms (Supplementary Table 6 and Supplementary Fig. 3). Furthermore, KEGG enrichment analysis revealed significant enrichments in the PPAR signaling pathway, insulin signaling pathway, PI3K-Akt signaling pathway, mTOR signaling pathway, MAPK signaling pathway, protein digestion and uptake pathways (Supplementary Table 7 and Supplementary Fig. 3). By analyzing genes within these enriched pathways, we identified a total of 12 genes (*ACADL*, *ACSL1*, *ADCY8*, *IGF1R*, *COL2A1*, *IGF1*, *OCLN*, *COL3A1*, *MTPN*, *PIK3CG*, *FASN*, and *BCAR1*) that exhibited significant associations with skeletal muscle growth, body size, carcass, and fat deposition. Among them, *COL3A1*, *IGF1*, *OCLN*, and *PIK3CG* in the turquoise module were identified as DEGs, which were highly and significantly correlated with body size and carcass phenotype; the *ACSL1* gene was in the brown module, which was highly considerably correlated with chest breadth and carcass weight. These results were

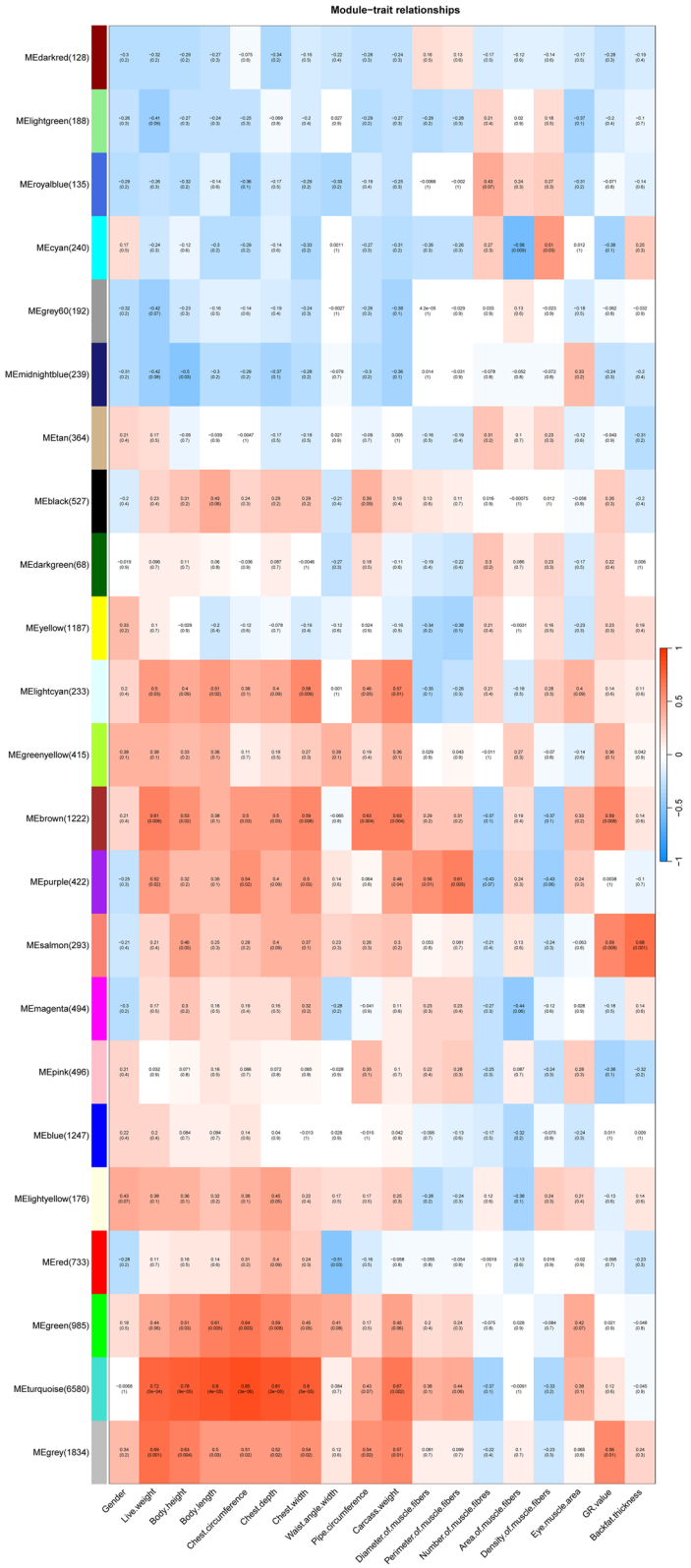

Fig. 8 Correlation analysis between modules and phenotypes. Vertical coordinate color blocks represent modules with the number of genes in parentheses, horizontal coordinates represent phenotypes, and the rightmost color bar represents the range of correlations. In the middle part of the heatmap, the darker the color, the higher the correlation; red means positive correlation, and blue means negative correlation; the numbers in each cell indicate correlation and significance

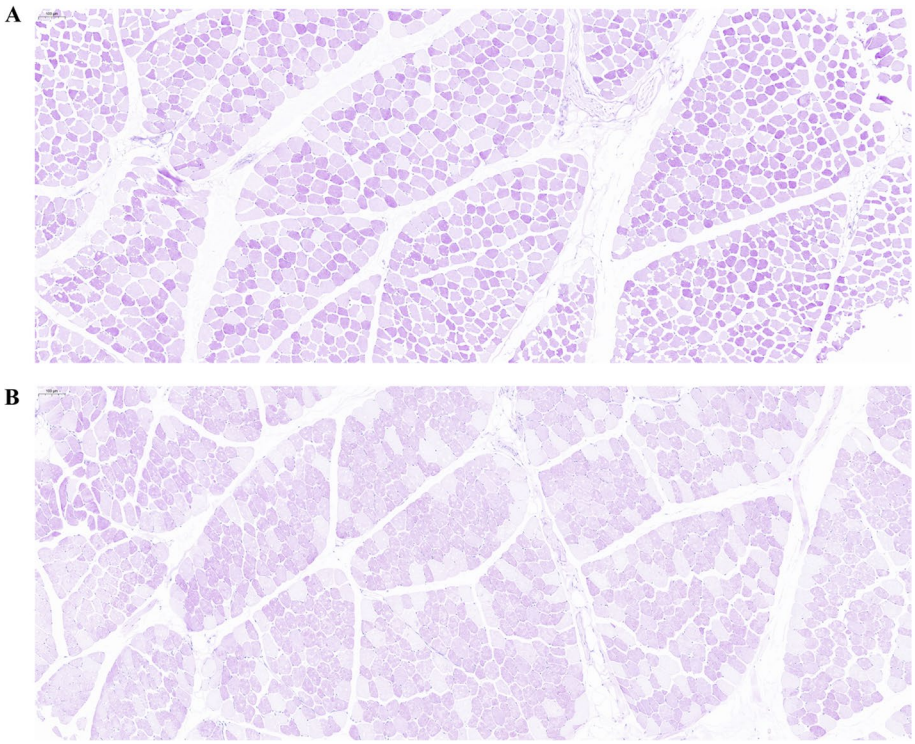

Fig. 9 Glycogen-stained sections of the longest dorsal muscle. A is PT PAS glycogen staining; B is ZS PAS glycogen staining. Note: Glycogen is purplish red with light blue nuclei

Table 6 Statistical analysis of glycogen staining results

Variety	Glycogen Positive area ratio(%)	N
PT	28.78 ± 14.28**	6
ZS	8.60 ± 9.33	6

The phenotypic values are the mean ± standard error (SE). P-values were calculated using a t-test. Superscript lowercase letters ** indicate highly significant differences ($P < 0.01$)

Table 7 FPKM values for module key genes

Gene	PT	ZS	Module
COL3A1	59.93 ± 17.12	86.82 ± 11.04	Turquoise
IGF1	1.71 ± 0.25	2.97 ± 0.45*	Turquoise
OCLN	0.29 ± 0.02	0.68 ± 0.07**	Turquoise
PIK3CG	0.27 ± 0.04	0.61 ± 0.09**	Turquoise

The FPKM values are the mean ± standard error (SE). Different superscript lowercase letters * within a row indicate significant differences at significance levels between $0.01 < P < 0.05$, and ** indicates significant differences at $P < 0.01$

consistent with previous studies on phenotypic data, further validating the reliability of this study.

Glycogen staining analysis

Transcriptome and WGCNA analyses revealed that many of the above genes are enriched regarding sugar metabolism and macromolecular metabolism processes, so we stained PT and ZS for glycogen. The results showed a significantly larger positive area for PT compared to ZS (Fig. 9 and Table 6). The DEGs of *IGF1*, *OCLN*, and *PIK3CG* in the transcriptome were downregulated genes, and the results of FPKM values for all three showed that ZS was higher than PT (Table 7). These consistent findings suggest that the involvement of *IGF1*, *OCLN*, and *PIK3CG* in the synthesis of myoglycogen may contribute to the muscular development and phenotypic characteristics of Tibetan sheep.

Discussion

In marker-assisted selection, the carcass can be enhanced by utilizing appropriate molecular markers that exhibit a significant positive influence on this trait [14]. Carcass characteristics are closely associated with factors such as muscle and bone growth and development. Notably, muscle tissue constitutes the largest proportion of animal carcasses and plays a crucial role in determining the production performance of livestock and poultry meat. Research has demonstrated that increasing muscle mass through hypertrophy inducers, such as insulin-like growth factor 1 (IGF-1), activates the PI3K/Akt signaling pathway, thereby promoting muscle growth [15]. Furthermore, skeletal muscle and muscle tissue are

strongly correlated with body size, which accounts for approximately 50% of body weight and is essential for the growth, development, and health status of animals [16]. Morphological evidence indicates that as body size increases, muscle tissue also expands accordingly. From the perspective of animal biochemical mechanisms, growth and development are driven by the metabolic activities of macromolecules such as carbohydrates, proteins, and lipids. Additionally, the concentration of myoglycogen, which provides critical energy support to muscles, increases with body size [17].

Body size traits

In the breeding research of meat sheep, body traits are considered one of the primary selection criteria and have garnered significant attention. Body size traits in meat sheep primarily encompass body weight, height, length, chest circumference, and pipe circumference etc. [18]. In the present research, ZS exhibited significantly higher live weight and measurements than PT, indicating that ZS demonstrated superior body size traits than PT.

Transcriptome and proteome analyses provide information on gene expression levels at the mRNA and protein levels, respectively. Integrating transcriptomics and proteomics data can yield a more comprehensive understanding of gene expression than histological data alone. The transcriptomics study identified *CTNNA3* [19, 20], *ADPRHL1* [21], *OCLN* [22], *KCNQ5* [23], and *COL3A1* [24], while the proteomics study revealed MYH15 [25], TMCO1 [26], ALB [27], ANPEP [28], UCP3 [29], ADIPOQ [30], and LDHA [31] as DEGs and DEPs. These DEGs and DEPs significantly affected animal growth, development, and phenotypic characteristics. *ALB* and *OCLN* were also identified in the combined analysis, and studies have reported that the *ALB* gene is associated with daily weight gain and affects sheep body weight by influencing fat deposition [27]. The *OCLN* gene was also screened in the WGCNA analysis, and previous studies have found that the expression of the OCLN protein in the jejunum of stunted piglets was lower than that of normal-growing piglets [22]. This study's findings align with those observed previously, suggesting that the *ALB* and *OCLN* genes may exert an influence on growth traits in Tibetan lineage sheep. The WGCNA is a systems biology approach that aims to describe patterns of association between genes and partition them into modules for further analysis. Unlike the Differential Expression Analysis, WGCNA considers inter-sample differences and gene relationships [32]. Both WGCNA and transcriptome analyses have unearthed the *COL3A1* gene, which may regulate skeletal development through modulation of gene expression, and skeletal development, including the development of length in various bones, exceptionally long bones, is critical for body size development [24]. The above study revealed that the *COL3A1* gene may be a candidate gene to influence the body size of Tibetan sheep.

Carcass traits

The carcass weight, slaughter rate, eye muscle area, backfat thickness, and GR values exhibited significant correlations with various production traits encompassing carcass characteristics and meat quality attributes [33]. The findings phenotypic measurements suggest that ZS exhibited superior carcass performance compared to PT. The characteristics of muscle fibers play a pivotal role in determining meat quantity, as they are a vital component of skeletal muscle and can significantly impact the overall biochemical and functional properties of muscle tissue, thereby influencing meat yield [34]. The comparison of muscle fiber characteristics suggests that ZS meat yield may exceed that of PT.

Transcriptional analyses revealed the differential expression of *MYOM2* [35], *DMD* [36], *AMPD1* [37], *TPM2* [38], *INSIG1* [39], and *PIK3CG* [40] genes, while proteomic analyses identified the altered abundance of ACACA [41], DYSF [42], TRIP11 [43], FLNC [44], ATP1A2 [45], and CAMK2B [46] proteins. These DEGs and DEPs regulate muscle growth and development and influence carcass weight, fat deposition, and metabolism. WGCNA analysis also identified the *PIK3CG* and *MTPN* genes, the *PIK3CG* gene associated with muscle development, phosphatidylinositol phosphorylation, and lipid binding [40]. In contrast, the *MTPN* gene promotes myotube hypertrophy increases myotube diameter, and promotes skeletal muscle cell differentiation and hypertrophy [47]. This provides new information on potential applications for improving beef yield. In addition, the *COL14A1* gene in the coanalysis, which was found to affect growth metabolism in Nellore cattle, carcass quality, and back fat thickness in pigs, was associated with preadipocyte to adipocyte differentiation as well as bone and muscle development [48]. These studies further proved the reliability of the present study that *PIK3CG*, *COL14A1*, *MTPN*, and *COL23A1* genes may play an essential role in carcass traits in Tibetan sheep.

Glycogen characteristics

Myoglycogen is the primary source of glucose for muscle glycolysis, which serves as the main substrate. Glycolysis is the most ancient metabolic pathway and plays a fundamental role in energy production across various living organisms. It also offers valuable molecular markers for the selective breeding of high-quality broiler strains [49]. The main compounds responsible for maintaining normal metabolism and function of skeletal muscle cells are

myoglycogen and glucose. Additionally, glycogen plays a role in influencing meat quality through its glycolytic potential [50]. In mammals, locomotor muscles typically consist of fast fiber types characterized by higher glycogen concentration, resulting in greater shortening velocities (v) and maximum shortening velocities (v_{max}) in smaller animals; however, the overall fiber composition becomes slower with lower glycogen concentration as body size increases [17]. The *IGF1* gene was highly expressed in the transcriptome, showed down-regulation in glycogen metabolic processes and monosaccharide transmembrane transport terminology, and was enriched in the PI3K-Akt signaling pathway and mTOR signaling pathway in WGCNA analysis. In the present investigation, we observed that the expression of this gene was significantly higher in ZS than in PT, while according to the phenotypic data, the glycogen content was lower and the body size was larger in ZS. The results of this study are consistent with previous findings. The *IGF1* gene has been demonstrated to exert an influence on growth and production traits across a range of livestock species, encompassing chickens, pigs, goats, sheep, and cattle. Furthermore, it also plays a role in determining body size and carcass characteristics specifically in sheep [51]. As a result of the above studies, the *IGF1* gene has an important role in determining body size and carcass traits in Tibetan lineage sheep.

The present study focuses on quantitative traits, which are complex traits regulated by multiple genes and therefore present a greater challenge for research. Furthermore, additional functional validation experiments are required to comprehensively elucidate the roles of the genes and proteins identified in this study. The findings presented herein will contribute to an enhanced comprehension of the growth and development patterns exhibited by Tibetan sheep, thereby facilitating advancements in their production performance and breeding novel high-yielding breeds.

Conclusions

Through comprehensive transcriptomic, proteomic, and WGCNA of the longest dorsal muscles in PT and ZS, this study identified 23 genes (including *MYOM2*, *AMPD1*, *OCLN*, *PIK3CG*, and *COL3A1* etc.) as well as proteins such as ACACA, DYSF, MYH15, TMCO1, TRIP11, ANPEP, UCP3, ALB, OCLN, FLNC, ATP1A2, ADIPOQ, LDHA, and CAMK2B. These genes and proteins are likely to influence sheep body shape characteristics and meat production performance by regulating critical biological processes, including muscle fibre formation and intramuscular fat deposition. These DEGs and DEPs may serve as potential novel biomarkers for predicting physical traits and meat production efficiency in sheep. We will prioritize the functional validation of these molecular markers in our future research endeavors.

Materials and methods

Statement of ethics

All animal experiments were carried out according to the procedures in the "Guidelines for Animal Care and Use" manual approved by the Animal Care and Use Committee of the Northwest Institute of Plateau Biology, Chinese Academy of Sciences (Approval No. NWIPB2023015). The animal owners gave informed consent to include all animals in the study.

Animals and sample collection

Nine healthy PT (four males and five females) and ten healthy ZS (five males and five females) were randomly selected from Qinghai Province, China. All animals were aged between 12 and 14 months. Before slaughter, the sheep underwent a fasting period of 12 h. Live weight and body measurements were recorded pre-slaughter, while carcass weight, backfat thickness, eye muscle area, and GR were measured post-slaughter. The longest dorsal muscles were collected immediately after slaughter and frozen in liquid nitrogen before storing at −80℃ degrees Celsius.

Muscle staining

The longest dorsal muscle samples were collected from all experimental animals post-slaughter. Subsequently, the samples were fixed with 4% paraformaldehyde, and then dehydrate in a series of ethanol. After upon achieving optimal fixation status, they underwent trimming, dehydration, embedding, sectioning, staining, and sealing processes. The resulting sections were examined using a PANORAMIC panoramic section scanner (DESK/MIDI/250/1000) to quantify the morphological characteristics of muscle fibers (e.g., diameter, area circumference density). This analysis was performed utilizing the scanning and viewing software Case Viewer 2.4. After imaging, five muscle fiber diameters, five muscle fiber circumferences, and five muscle fiber perimeters were quantified in each section using Image-Pro Plus 6.0 analysis software, followed by calculating the mean values. The number of muscle fibers was enumerated in each section, and the corresponding total muscle fiber area was measured to determine the muscle fiber density (number of muscle fibers/total muscle fiber area). A total of 19 samples of muscle tissue were analyzed, including nine from PT and ten from ZS.

Library preparation and RNA-seq

Total RNA was purified using Trizol Reagent (Invitrogen Life Technologies), followed by the determination of

RNA quantity and quality using NanoDrop spectrophotometer (Thermo Scientific, Waltham, Massachusetts, USA), and RNA integrity using Agilent 2100. The NEBNext Ultra II RNA Library Prep Kit for Illumina (New England Biolabs Inc; Ipswich, Massachusetts, USA) was used to enrich mRNAs with polyA tails through Oligo (dT) magnetic beads, followed by random fragmentation using divalent cations. Double-stranded cDNA was purified, followed by double-end repair and the introduction of the "A" base at the 3' end, along with the ligation of the sequencing junction. The cDNA was size-selected using AMPure XP beads targeting approximately 400–500 bp fragments. After PCR amplification and purification, the quality of the constructed sequencing library was measured-Agilent High Sensitivity DNA Analysis on a Bioanalyzer 2100 system (Agilent). Finally, libraries were sequenced on an Illumina NovaSeq 6000 platform.

RNA-seq analysis

Raw sequencing data were filtered via fastp [52] to remove low-quality reads (< Q20). The clean data were mapped to the reference genome (GCF_016772045.1_ARS-UI_Ramb_v2.0) using HISAT2 v2.0.5 [53]. The read counts for each gene were quantified using HTSeq (0.9.1) [54], and gene expression values were calculated based on the measurement of FPKM > 1.

The DESeq software (version 1.20.0) [55] was used to analyze differential expressions between the two groups. DEGs were defined based on the criteria of a P-value less than 0.05 and a $\log_2$Fold Change (FC) indicating significant diversity in expression differences greater than one.

The topGO package and Clusterprofiler (3.4.4) software [56] were utilized for GO and KEGG analyses. GO terms and pathways with p values less than 0.05 were significantly enriched.

Sample preparation and tissue protein extraction

Twenty samples were individually ground in liquid nitrogen, and the appropriate amount of SDT lysate was added. The mixture was then transferred to an EP tube and subjected to a boiling water bath for 3 min, followed by ultrasonic crushing for 2 min. The supernatant was extracted after centrifugation at 16000 g for 20 min at 4℃. The resulting supernatant was collected and quantified using the BCA Protein Assay Kit (BeyoTime, China). Then, each sample's appropriate amount of protein was subjected to FASP digestion. After digestion, the peptide was desalted by a C18 cartridge and freeze-dried under a vacuum. The peptides were dried and reconstituted with 0.1% FA, and the peptide concentration was determined for LC–MS analysis.

LC–MS/MS and data analysis

The LC–MS/MS analysis was conducted using an Orbitrap Astral mass spectrometry system coupled with a Vanquish Neo UHPLC system (Thermo Fisher Scientific). An appropriate amount of peptide was taken from each sample, and chromatographic separation was performed using the Vanquish Neo UHPLC system, operated Neo UHPLC chromatography system (Thermo Scientific). Buffers: solution A was 0.1% formic acid aqueous solution, and solution B was 0.1% formic acid acetonitrile aqueous solution (acetonitrile 80%). The chromatographic column was equilibrated with 96% of A solution. The samples were injected into a Trap Column (PepMap Neo 5 μm C18 300 μm X 5 mm, Thermo Scientific) and then passed through a chromatographic analytical column (μ PAC Neo High Throughput column, Thermo Scientific) for gradient separation. DIA (data-independent acquisition) mass spectrometry separated and analyzed the peptides using an Orbitrap Astral mass spectrometer (Thermo Scientific). The analysis time was 15 min.

The DIA MS data were analyzed using the DIA-NN 1.8.1 software [57, 58]. The database is uniprotkb-Ovis aries-[9940]−48903–20231012. fasta, from the URL https://www.uniprot.org/taxonomy/9940, its protein entry: 48,903, downloaded on 2023–10.

The commonly employed approach in protein difference analysis involves utilizing the t-test and FC, representing the ratio of mean expression values between two groups, to identify significantly different proteins. Typically, these proteins are identified based on meeting criteria such as a p-value < 0.05 and FC > 1.5 or < 1/1.5. However, if an unrepeated sample group is present, the significance of the p-value is not considered.

Bioinformatic analysis

The volcano plots of DEGs were generated using the ggplots2 package in R. Heatmaps were conducted using the Pheatmap package in R. To annotate the peptide sequences, relevant information was extracted from UniProtKB/Swiss-Prot [59], KEGG [60], and GO. The GO and KEGG enrichment analyses were conducted using Fisher's exact test with FDR correction for multiple tests. GO terms were categorized into three groups: biological process (BP), molecular function (MF), and cellular component (CC) [61].

Correlation analysis of the transcriptomes and proteomes

Pearson's correlation coefficient (R) was calculated between the transcriptome and proteome data based on $\log_2$FC. Subsequently, scatter plots were generated

for visualization purposes. A threshold of $R > 0.80$ was considered statistically significant to establish a strong correlation between these datasets [62–65].

RT-qPCR validation of DEGs

The total RNA was extracted using the RNA extraction solution (Wuhan Servicebio Technology Co., Ltd, G3013, Wuhan, China), followed by cDNA synthesis using the reverse transcription kit item G3337. Reverse transcription reaction system preparation: The total reaction volume was 20μL, comprising 4μL of 5×SweScript All-in-One SuperMix for qPCR, 1μL of gDNA Remover, 10μL of Total RNA, and 5μL of Nuclease-Free Water. Gently mix the reagents and perform a brief centrifugation. Amplification was performed on a fluorescence quantitative PCR instrument (CFX Connect, Bio-rad). The amplification process consisted of three steps: predenaturation at 95 °C for 30 s; denaturation at 95 °C for 15 s, and annealing at 60 °C for 30 s during each cycle repeated for a total of 40 cycles; and finally, temperature ranging from 65 °C to 95 °C with fluorescence signals collected every increment of 0.5 °C in temperature increase. The technical replication was performed three times, utilizing SYBR Green as the fluorescence quantification reagent. Specific primers were designed for the selected genes using Primer5 software, with the sheep *GAPDH* gene as the internal reference gene (Supplementary Table 8). Each RT-qPCR reaction was independently replicated three times. The results were used to calculate the relative expression of each gene through the $2^{-\Delta\Delta CT}$ method [66]. Ultimately, the Pearson correlation coefficient calculation determined the correlation between transcriptome and RT-qPCR gene expression.

Weighted gene co-expression network analysis

Following the WGCNA method proposed by Langfelder and Horvath in 2008, we utilized the WGCNA package to construct co-expression networks for all samples. The WGCNA package offers a comprehensive set of functions for network construction, module identification, gene selection, calculation of topological properties, data simulation, and visualization. Additionally, it provides interfaces for integration with external software packages [67]. In this study, the pick soft threshold function was employed to assess the network topology at various soft thresholds, aiding in determining the optimal soft threshold power. Additionally, we opted to include all available data for analysis.

Glycogen staining

Firstly, 12 muscle tissue samples of PT (3 rams and 3 ewes) and ZS (3 rams and 3 ewes) were taken for the preparation of tissue sections, including fixation, embedded paraffin sections, frozen sections, and other SOP preparations for the experiments. Then the paraffin sections were dewaxed with water, and frozen sections were rewarmed and fixed, sliced into PAS staining solution, followed by dehydration and sealing, and finally, microscopic microscopy and image acquisition for analysis. Based on the HALO platform of Indica labs (U.S.A), positive area and tissue area analyses were performed on scans of special stains, including the selection of the target area, the selection of the analysis module, the selection of the colors, the calculations and analyses, and finally the calculation of the positive area ratio (positive area/tissue area).

Abbreviations

ACACA	Acetyl-CoA carboxylase alpha
ACADL	Acyl-CoA dehydrogenase long chain
ACSL1	Acyl-CoA synthetase long chain family member 1
ADCY8	Adenylate cyclase 8
ADIPOQ	Adiponectin, C1Q and collagen domain containing
ADPRHL1	ADP-ribosylhydrolase like 1
AHCYL2	Adenosylhomocysteinase like 2
ALB	Albumin
AMPD1	Adenosine monophosphate deaminase 1
ANPEP	Alanyl aminopeptidase, membrane
ATP1 A2	ATPase Na+/K+ transporting subunit alpha 2
BCAR1	BCAR1 scaffold protein, Cas family member
C25H10orf71	Chromosome 25 C10orf71 homolog
C8B	Complement C8 beta chain
CAMK2B	Calcium/calmodulin dependent protein kinase II beta
CD200	CD200 molecule
COL14 A1	Collagen type XIV alpha 1 chain
COL23 A1	Collagen type XXIII alpha 1 chain
COL2 A1	Collagen type II alpha 1 chain
COL3 A1	Collagen type III alpha 1 chain
CSRP3	Cysteine and glycine rich protein 3
CTNNA3	Catenin alpha 3
CYB5 A	Cytochrome b5 type A
DMD	Dystrophin
DYSF	Dysferlin
EYA1	EYA transcriptional coactivator and phosphatase 1
F9	Coagulation factor IX
FASN	Fatty acid synthase
FLNC	Filamin C
GAPDH	Glyceraldehyde-3-phosphate dehydrogenase
IGF1	Insulin like growth factor 1
IGF1R	Insulin like growth factor 1 receptor
ILK	Integrin linked kinase
INSIG1	Insulin induced gene 1
KCNQ5	Potassium voltage-gated channel subfamily Q member 5
KIF4 A	Kinesin family member 4A
LDHA	Lactate dehydrogenase A
MLIP	Muscular LMNA interacting protein
MTPN	Myotrophin
MYH15	Myosin heavy chain 15
MYOM2	Myomesin 2
MYOM3	Myomesin 3
NCKAP5	NCK associated protein 5
OCLN	Occludin
PADI2	Peptidyl arginine deiminase 2
PIK3 CG	Phosphatidylinositol-4,5-bisphosphate 3-kinase catalytic subunit gamma
PON1	Paraoxonase 1
PT	Plateau-type Tibetan sheep
QSOX1	Quiescin sulfhydryl oxidase 1
SMTNL1	Smoothelin like 1

TMCO1	Transmembrane and coiled-coil domains 1
TNC	Tenascin C
TPM2	Tropomyosin 2
TRIP11	Thyroid hormone receptor interactor 11
UCP3	Uncoupling protein 3
WGCNA	Weighted gene co-expression network analysis
ZS	Zhashijia sheep

Supplementary Information

The online version contains supplementary material available at https://doi.org/10.1186/s12864-025-11738-z.

Supplementary Material 1. Supplementary Fig. 1: Venn diagram of transcriptome DEGs and proteome DEPs. Supplementary Fig. 2: WGCNA analysis. Supplementary Fig. 3: The gene GO and KEGG enrichment analysis.

Supplementary Material 2. Supplementary Table 1: RNAseq Map. Supplementary Table 2: GO term enrichment analysis of DEGs. Supplementary Table 3: KEGG pathway enrichment analysis of DEGs. Supplementary Table 4: GO term enrichment analysis of DEPs. Supplementary Table 5: KEGG pathway enrichment analysis of DEPs. Supplementary Table 6: The gene GO enrichment analysis. Supplementary Table 7: The gene KEGG enrichment analysis. Supplementary Table 8: Parameters of primer pairs used for RT-qPCR.

Acknowledgements
Not applicable.

Authors' contributions
DT conceived and designed the experiments. DL analyzed the data and wrote the paper. FT revised manuscript. KZ provided essential suggestions. LW, QP, JZ, DS, QR, HJ, WZ, RL, and GB participated in the data collection. BH, XL, SL, and SW performed the experiments. All authors read and approved the final manuscript.

Funding
This study was supported by the Natural Science Foundation of Qinghai Province [2022-ZJ-901]; National Breeding Joint Research Project; and Dr. Kai Zhao was supported by the "Kunlun talent" project of Qinghai Province.

Data availability
The Transcriptome and Proteome data have been deposited to the NCBI (PRJNA1136802) and iProX (PXD054235), respectively.

Declarations

Ethics approval and consent to participate
The animal experiments were conducted in accordance with the procedures outlined in the "Guidelines for Animal Care and Use" manual, which was approved by the Animal Care and Use Committee of the Northwest Institute of Plateau Biology, Chinese Academy of Sciences (Approval No. NWIPB2023015). Informed consent was obtained from the animal owners to include all animals in this study.

Consent for publication
Not applicable.

Competing interests
The authors declare no competing interests.

Author details
[1]Qinghai Provincial Key Laboratory of Animal Ecological Genomics, Key Laboratory of Adaptation and Evolution of Plateau Biota, Northwest Institute of Plateau Biology, Chinese Academy of Sciences, No. 23 Xining Road, Xining, Qinghai 810001, China. [2]University of Chinese Academy of Sciences, Beijing 100049, China. [3]Qinghai Sheep Breeding and Promotion Service Center, Gangcha, Qinghai 812300, China. [4]Branch of Animal Husbandry and Veterinary of Heilongjiang Academy of Agricultural Sciences, Qiqihar 161005, China. [5]Qinghai Livestock and Poultry Genetic Resources Protection and Utilization Center, Xining 810000, China. [6]Animal Husbandry and Veterinary Station of Huzhu County of Qinghai Province, Huzhu 810500, Qinghai, China. [7]Minhe County Zongbao Township Animal Husbandry and Veterinary Station, Minhe, Qinghai 810800, China. [8]Minhe County Machangyuan Township Animal Husbandry and Veterinary Station, Minhe, Qinghai 810800, China.

Received: 21 January 2025 Accepted: 21 May 2025
Published online: 29 May 2025

References

1. Guo Q. Test of meat performance and estimation of genetic parameters of growth traits in Dorper×Hu hybrid sheep. Shanxi Agricultural University. 2019:40–50. https://doi.org/10.27285/d.cnki.gsxnu.2019.000213.
2. Liu X, Xiong X, Yang J, Zhou L, Yang B, Ai H, Ma H, Xie X, Huang Y, Fang S, Xiao S, Ren J, Ma J, Huang L. Genome-wide association analyses for meat quality traits in Chinese Erhualian pigs and a Western Duroc × (Landrace × Yorkshire) commercial population. Genet Sel Evol. 2015;47(1):44.
3. Liu D, Li X, Wang L, Pei Q, Zhao J, Sun D, Ren Q, Tian D, Han B, Jiang H, Zhang W, Wang S, Tian F, Liu S, Zhao K. Genome-wide association studies of body size traits in Tibetan sheep. BMC Genomics. 2024;25(1):739.
4. Wang Z, Zhang X, Liu Y, Pei S, Kong Y, Li F, Wang W, Yue X. Preliminary genetic parameter estimates of meat quality traits in Hu sheep. Meat Sci. 2024;212: 109476.
5. Montossi F, Font-i-Furnols M, del Campo M, San Julián R, Brito G, Sañudo C. Sustainable sheep production and consumer preference trends: compatibilities, contradictions, and unresolved dilemmas. Meat Sci. 2013;95(4):772–89.
6. Zhao D. Identification of key genes for carcass traits in Tiannong partridge chickens based on transcriptome. Foshan University. 2022:1–5. https://doi.org/10.27960/d.cnki.gfskj.2022.000320.
7. Shi Huibin. Whole genome resequencing reveals genetic diversity and selection signals in Panou sheep selection breeding population. Gansu Agriculture University. 2023:1–4. https://doi.org/10.27025/d.cnki.ggsnu.2023.000051.
8. Liu Y, Zhang X, Wang K, Li Q, Yan S, Shi H, Liu L, Liang S, Yang M, Su Z, Ge C, Jia J, Xu Z, Dou T. RNA-Seq reveals pathways responsible for meat quality characteristic differences between two yunnan indigenous chicken breeds and commercial broilers. Foods. 2024;13(13): 2008.
9. Ding H, Lin Y, Zhang T, Chen L, Zhang G, Wang J, Xie K, Dai G. Transcriptome analysis of differentially expressed mRNA related to Pigeon muscle development. Animals (Basel). 2021;11(8):2311.
10. Zhao L, Zhang D, Li X, Zhang Y, Zhao Y, Xu D, Cheng J, Wang J, Li W, Lin C, Yang X, Ma Z, Cui P, Zhang X, Wang W. Comparative proteomics reveals genetic mechanisms of body weight in Hu sheep and Dorper sheep. J Proteomics. 2022;267: 104699.
11. Ponomarenko EA, Krasnov GS, Kiseleva OI, Kryukova PA, Arzumanian VA, Dolgalev GV, Ilgisonis EV, Lisitsa AV, Poverennaya EV. Workability of mRNA Sequencing for Predicting Protein Abundance. Genes (Basel). 2023;14(11): 2065.
12. Lou X, Wang H, Ni X, Gao Z, Iqbal S. Integrating proteomic and transcriptomic analyses of loquat (Eriobotrya japonica Lindl.) in response to cold stress. Gene. 2018;677:57–65.
13. Zhang HY, Lei G, Zhou HW, He C, Liao JL, Huang YJ. Quantitative iTRAQ-based proteomic analysis of rice grains to assess high night temperature stress. Proteomics. 2017;17(5):1600365.
14. Grochowska E, Lisiak D, Akram MZ, Adeniyi OO, Lühken G, Borys B. Association of a polymorphism in exon 3 of the IGF1R gene with growth, body size, slaughter and meat quality traits in Colored Polish Merino sheep. Meat Sci. 2021;172: 108314.
15. Glass DJ. Skeletal muscle hypertrophy and atrophy signaling pathways. Int J Biochem Cell Biol. 2005;37(10):1974–84.
16. Hu Z, Cao J, Ge L, Zhang J, Zhang H, Liu X. Characterization and Comparative Transcriptomic Analysis of Skeletal Muscle in Pekin Duck at Different Growth Stages Using RNA-Seq. Animals (Basel). 2021;11(3):834.
17. Cieri RL, Dick TJM, Morris JS, Clemente CJ. Scaling of fibre area and fibre glycogen concentration in the hindlimb musculature of monitor lizards: implications for locomotor performance with increasing body size. J Exp Biol. 2022;225(Suppl_1):jeb243380.

18. Huang Z. Analysis of MYLK4 and MTPN gene polymorphisms and their association with growth traits in different breeds of sheep. Northwest Minzu University. 2023:1–3. https://doi.org/10.27408/d.cnki.gxmzc.2023.000459.
19. Zhao L, Li F, Yuan L, Zhang X, Zhang D, Li X, Zhang Y, Zhao Y, Song Q, Wang J, Zhou B, Cheng J, Xu D, Li W, Lin C, Wang W. Expression of ovine CTNNA3 and CAP2 genes and their association with growth traits. Gene. 2022;807: 145949.
20. Yu H, Yu S, Guo J, Cheng G, Mei C, Zan L. Genome-Wide Association Study Reveals Novel Loci Associated with Body Conformation Traits in Qinchuan Cattle. Animals (Basel). 2023;13(23):3628.
21. Li T, Chen B, Wei C, Hou D, Qin P, Jing Z, Ma H, Niu X, Wang C, Han R, Li H, Liu X, Xu H, Kang X, Li Z. A 104-bp Structural Variation of the ADPRHL1 Gene Is Associated With Growth Traits in Chickens. Front Genet. 2021;12: 691272.
22. Su W, Zhang H, Ying Z, Li Y, Zhou L, Wang F, Zhang L, Wang T. Effects of dietary L-methionine supplementation on intestinal integrity and oxidative status in intrauterine growth-retarded weanling piglets. Eur J Nutr. 2018;57(8):2735–45.
23. Zeng H, Zhong Z, Xu Z, Teng J, Wei C, Chen Z, Zhang W, Ding X, Li J, Zhang Z. Meta-analysis of genome-wide association studies uncovers shared candidate genes across breeds for pig fatness trait. BMC Genomics. 2022;23(1):786.
24. Doyle JL, Berry DP, Veerkamp RF, Carthy TR, Evans RD, Walsh SW, Purfield DC. Genomic regions associated with muscularity in beef cattle differ in five contrasting cattle breeds. Genet Sel Evol. 2020;52(1):2.
25. Bolormaa S, Pryce JE, Reverter A, Zhang Y, Barendse W, Kemper K, Tier B, Savin K, Hayes BJ, Goddard ME. A multi-trait, meta-analysis for detecting pleiotropic polymorphisms for stature, fatness and reproduction in beef cattle. PLoS Genet. 2014;10(3): e1004198.
26. Duan X, An B, Du L, Chang T, Liang M, Yang BG, Xu L, Zhang L, Li J, E G, Gao H. Genome-wide association analysis of growth curve parameters in chinese simmental Beef Cattle. Animals (Basel). 2021;11(1):192.
27. Zhao L, Wang W, Wang X, Zhang D, Li X, Zhao Y, Zhang Y, Xu D, Cheng J, Wang J, Li W, Lin C, Wu W, Zhang X, Zheng W. Identification of SNPs and expression patterns of ALB, AHSG and GC genes and their association with growth traits in Hu sheep. Gene. 2023;853: 147100.
28. Wang X, Xiao Y, Yang H, Lu L, Liu X, Lyu W. Transcriptome analysis reveals the genes involved in growth and metabolism in muscovy ducks. Biomed Res Int. 2021;2021: 6648435.
29. Cheng J, Zhang X, Li F, Yuan L, Zhang D, Zhang Y, Song Q, Li X, Zhao Y, Xu D, Zhao L, Li W, Wang J, Zhou B, Lin C, Yang X, Wang W. Detecting single nucleotide polymorphisms in MEF2B and UCP3 and elucidating their association with sheep growth traits. DNA Cell Biol. 2021;40(12):1554–62.
30. Wang L, Xue K, Wang Y, Niu L, Li L, Zhong T, Guo J, Feng J, Song T, Zhang H. Molecular and functional characterization of the adiponectin (AdipoQ) gene in goat skeletal muscle satellite cells. Asian-Australas J Anim Sci. 2018;31(8):1088–97.
31. Qiu H, Xu X, Fan B, Rothschild MF, Martin Y, Liu B. Investigation of LDHA and COPB1 as candidate genes for muscle development in the MYOD1 region of pig chromosome 2. Mol Biol Rep. 2010;37(1):629–36.
32. Wang J, Chen H, Zeng X. Identification of hub genes associated with follicle development in multiple births sheep by WGCNA. Front Vet Sci. 2022;9: 1057282.
33. Zhang Y, Zhang J, Gong H, Cui L, Zhang W, Ma J, Chen C, Ai H, Xiao S, Huang L, Yang B. Genetic correlation of fatty acid composition with growth, carcass, fat deposition and meat quality traits based on GWAS data in six pig populations. Meat Sci. 2019;150:47–55.
34. Deng K, Liu Z, Su Y, Fan Y, Zhang Y, Wang F. Comparison of muscle fiber characteristics and meat quality between newborn and adult Haimen goats. Meat Sci. 2024;207: 109361.
35. Moreno-Sánchez N, Rueda J, Carabaño MJ, Reverter A, McWilliam S, González C, Díaz C. Skeletal muscle specific genes networks in cattle. Funct Integr Genomics. 2010;10(4):609–18.
36. Xu S, Chang Y, Wu G, Zhang W, Man C. Potential role of miR-155-5p in fat deposition and skeletal muscle development of chicken. Biosci Rep. 2020;40(6):BSR20193796.
37. Shao M, Shi K, Zhao Q, Duan Y, Shen Y, Tian J, He K, Li D, Yu M, Lu Y, Tang Y, Feng C. Transcriptome analysis reveals the differentially expressed genes associated with growth in Guangxi Partridge Chickens. Genes (Basel). 2022;13(5): 798.
38. Wang Z, Shang P, Li Q, Wang L, Chamba Y, Zhang B, Zhang H, Wu C. iTRAQ-based proteomic analysis reveals key proteins affecting muscle growth and lipid deposition in pigs. Sci Rep. 2017;7: 46717.
39. Bionaz M, Loor JJ. Gene networks driving bovine milk fat synthesis during the lactation cycle. BMC Genomics. 2008;9: 366.
40. Liu H, Hou L, Zhou W, Wang B, Han P, Gao C, Niu P, Zhang Z, Li Q, Huang R, Li P. Genome-Wide Association Study and FST Analysis Reveal Four Quantitative Trait Loci and Six Candidate Genes for Meat Color in Pigs. Front Genet. 2022;13: 768710.
41. Bakhtiarizadeh MR, Alamouti AA. RNA-Seq based genetic variant discovery provides new insights into controlling fat deposition in the tail of sheep. Sci Rep. 2020;10(1):13525.
42. Xu T, Xu F, Gu L, Rong G, Li M, Qiao F, Shi L, Wang D, Xia W, Xun W, Cao T, Liu Y, Lin Z, Zhou H. Landscape of alternative splicing in Capra_hircus. Sci Rep. 2018;8(1):15128.
43. Xue Y, Liu S, Li W, Mao R, Zhuo Y, Xing W, Liu J, Wang C, Zhou L, Lei M, Liu J. Genome-wide association study reveals additive and non-additive effects on growth traits in duroc pigs. Genes (Basel). 2022;13(8):1454.
44. Zheng C, Zhong Y, Zhang P, Guo Q, Li F, Duan Y. Dynamic transcriptome profiles of skeletal muscle growth and development in Shaziling and Yorkshire pigs using RNA-sequencing. J Sci Food Agric. 2024;104(12):7301–14.
45. Feng L, Si J, Yue J, Zhao M, Qi W, Zhu S, Mo J, Wang L, Lan G, Liang J. The landscape of accessible chromatin and developmental transcriptome maps reveal a genetic mechanism of skeletal muscle development in pigs. Int J Mol Sci. 2023;24(7): 6413.
46. Yang G, Wu M, Liu X, Wang F, Li M, An X, Bai F, Lei C, Dang R. MiR-24-3p conservatively regulates muscle cell proliferation and apoptosis by targeting common gene CAMK2B in Rat and Cattle. Animals (Basel). 2022;12(4):505.
47. Bordbar F, Jensen J, Du M, Abied A, Guo W, Xu L, Gao H, Zhang L, Li J. Identification and validation of a novel candidate gene regulating net meat weight in Simmental beef cattle based on imputed next-generation sequencing. Cell Prolif. 2020;53(9): e12870.
48. Shangguan A, Xiang C, Deng Z, Zhang N, Yu M, Zhang F, Suo X, Chen M, Chen C, Tao H, Xiong Q. Genome-wide association study of growth and reproductive traits based on low-coverage whole-genome sequencing in a Chubao black-head goat population. Gene. 2024;931: 148891.
49. Liu X, Liu L, Wang J, Cui H, Chu H, Bi H, Zhao G, Wen J. Genome-wide association study of muscle glycogen in Jingxing Yellow Chicken. Genes (Basel). 2020;11(5):497.
50. Essén-Gustavsson B, Jensen-Waern M, Jonasson R, Andersson L. Effect of exercise on proglycogen and macroglycogen content in skeletal muscles of pigs with the Rendement Napole mutation. Am J Vet Res. 2005;66(7):1197–201.
51. Kader Esen V, Esen S. Association of the IGF1 5'UTR Polymorphism in Meat-Type Sheep Breeds Considering Growth, Body Size, Slaughter, and Meat Quality Traits in Turkey. Vet Sci. 2023;10(4):270.
52. Chen S, Zhou Y, Chen Y, Gu J. fastp: an ultra-fast all-in-one FASTQ preprocessor. Bioinformatics. 2018;34(17):i884–90.
53. Kim D, Paggi JM, Park C, Bennett C, Salzberg SL. Graph-based genome alignment and genotyping with HISAT2 and HISAT-genotype. Nat Biotechnol. 2019;37(8):907–15.
54. Anders S, Pyl PT, Huber W. HTSeq–a Python framework to work with high-throughput sequencing data. Bioinformatics. 2015;31(2):166–9.
55. Anders S, Huber W. Differential expression analysis for sequence count data. Genome Biol. 2010;11(10): R106.
56. Yu G, Wang LG, Han Y, He QY. clusterProfiler: an R package for comparing biological themes among gene clusters. OMICS. 2012;16(5):284–7.
57. Demichev V, Messner CB, Vernardis SI, Lilley KS, Ralser M. DIA-NN: neural networks and interference correction enable deep proteome coverage in high throughput. Nat Methods. 2020;17(1):41–4.
58. Barkovits K, Pacharra S, Pfeiffer K, Steinbach S, Eisenacher M, Marcus K, Uszkoreit J. Reproducibility, specificity and accuracy of relative quantification using spectral library-based data-independent acquisition. Mol Cell Proteomics. 2020;19(1):181–97.
59. Boutet E, Lieberherr D, Tognolli M, Schneider M, Bansal P, Bridge AJ, Poux S, Bougueleret L, Xenarios I. UniProtKB/Swiss-Prot, the Manually

Annotated Section of the UniProt KnowledgeBase: How to Use the Entry View. Methods Mol Biol. 2016;1374:23–54.
60. Kanehisa M, Goto S, Sato Y, Furumichi M, Tanabe M. KEGG for integration and interpretation of large-scale molecular data sets. Nucleic Acids Res. 2012;40(Database issue):D109-14.
61. Ashburner M, Ball CA, Blake JA, Botstein D, Butler H, Cherry JM, Davis AP, Dolinski K, Dwight SS, Eppig JT, Harris MA, Hill DP, Issel-Tarver L, Kasarskis A, Lewis S, Matese JC, Richardson JE, Ringwald M, Rubin GM, Sherlock G. Gene ontology: tool for the unification of biology. Gene Ontol Consort Nat Genet. 2000;25(1):25–9.
62. de Winter JC, Gosling SD, Potter J. Comparing the Pearson and Spearman correlation coefficients across distributions and sample sizes: A tutorial using simulations and empirical data. Psychol Methods. 2016;21(3):273–90.
63. Warrens MJ. Transforming intraclass correlation coefficients with the Spearman-Brown formula. J Clin Epidemiol. 2017;85:14–6.
64. Ma Q, Liu X, Feng W, Liu S, Zhuang Z. Analyses of the molecular mechanisms associated with salinity adaption of Trachidermus fasciatus through combined iTRAQ-based proteomics and RNA sequencing-based transcriptomics. Prog Biophys Mol Biol. 2018;136:40–53.
65. Zhao L, Li F, Zhang X, Zhang D, Li X, Zhang Y, Zhao Y, Song Q, Huang K, Xu D, Cheng J, Wang J, Li W, Lin C, Wang W. Integrative analysis of transcriptomics and proteomics of longissimus thoracis of the Hu sheep compared with the Dorper sheep. Meat Sci. 2022;193: 108930.
66. Livak KJ, Schmittgen TD. Analysis of relative gene expression data using real-time quantitative PCR and the 2(-Delta Delta C(T)) Method. Methods. 2001;25(4):402–8.
67. Langfelder P, Horvath S. WGCNA: an R package for weighted correlation network analysis. BMC Bioinform. 2008;9:559.

Publisher's Note